

Contents lists available at ScienceDirect

Petroleum Science

journal homepage: www.keaipublishing.com/en/journals/petroleum-science



Structural determinants of asphaltenes behavior: Heteroatom-driven aggregation dynamics and viscosity enhancement in heavy oil systems



Guan-Dong Wang ^a, Peng-Cheng Zou ^a, Si-Si Cheng ^a, Yong Hu ^b, Xue-Yu Wang ^{a,*}, Ji-Chao Fang ^{b,**}

- ^a College of Geography and Environmental Sciences, Zhejiang Normal University, Jinhua, 321000, Zhejiang, China
- ^b Petroleum Exploration and Production Research Institute, SINOPEC, Beijing, 102206, China

ARTICLE INFO

Article history: Received 11 March 2025 Received in revised form 20 May 2025 Accepted 30 July 2025 Available online 7 August 2025

Edited by Min Li

Keywords:
Heteroatom
Asphaltene morphology
Self-assembly
Adsorption mechanism
Heavy oil viscosity
Molecular dynamics simulation

ABSTRACT

Heavy oil, constituting a significant portion of global oil reserves, presents unique challenges in extraction and processing due to its high viscosity, largely influenced by asphaltenes and their heteroatom content. This study employs molecular dynamics (MD) simulations to investigate the selfaggregation and adsorption mechanisms of heteroatom/non-heteroatom asphaltenes, comparing linear and island structural configurations. Key findings reveal that linear heteroatom asphaltenes form dense, multi-layered aggregates, while island heteroatom asphaltenes exhibit stronger aggregation energy. On solid surfaces, linear asphaltenes display multi-layered adsorption, whereas island asphaltenes adopt a dispersed structure with higher adsorption energy, making them more resistant to removal. Compared to non-heteroatom asphaltenes, heteroatom asphaltenes significantly enhance the aggregation energy of the asphaltene itself and the interaction energy with light oil components, reducing the diffusion capacity of oil droplets and increasing viscosity. Although the viscosity of island heteroatom asphaltene oil drops is the largest, the role of heteroatom in linear asphaltene is more obvious, and linear heteroatom asphaltene and non-heteroatom show great differences in properties. Additionally, heteroatom-containing oil droplets exhibit stronger interactions with solid surfaces, driven by the influence of heteroatom asphaltenes on lighter oil components. These insights provide a deeper understanding of heavy oil viscosity mechanisms, offering a foundation for developing targeted viscosity-reduction strategies and optimizing heavy oil recovery and processing techniques.

© 2025 The Authors. Publishing services by Elsevier B.V. on behalf of KeAi Communications Co. Ltd. This is an open access article under the CC BY license (http://creativecommons.org/licenses/by/4.0/).

1. Introduction

Heavy oil is pivotal and inescapable in the global oil resources panorama (Kober et al., 2020; Seidy-Esfahlan et al., 2024). By the conclusion of 2020, the world's cumulative proven oil reserves had reached an impressive 1.732 trillion barrels, with heavy oil constituting a substantial 40% of the global reserves (BP, 2024; Temizel et al., 2016). As traditional sources of light oil continue to diminish and energy needs rise, it is increasingly crucial to

Peer review under the responsibility of China University of Petroleum (Beijing).

efficiently exploit heavy oil to advance our society's development (Schüppel and Gräbner, 2024; Yatimi et al., 2024). The path of heavy oil development and utilization is fraught with numerous challenges, and the pursuit of efficient and rational mining methods has emerged as the new focus of research (Shahzad et al., 2024; Sun et al., 2024; Xiong et al., 2024). Traditional mining methods, such as electromagnetic heating (Bera and Babadagli, 2015), steam flooding (Zhang et al., 2023), and steam huff and puff (Wang et al., 2022), are beset by high costs, low efficiency, and unstable exploitation. Conversely, chemical cold recovery has emerged as a promising alternative in recent years (Ren et al., 2024; Xu F. et al., 2020; Xu Y. et al., 2020). Evidence has indicated that chemical cold recovery can boost the heavy-oil recovery rate to a range of 42%–88% (Coskuner et al., 2015). A more profound understanding of heavy-oil viscosity mechanisms is essential for

^{*} Corresponding author.

^{**} Corresponding author.

E-mail addresses: xywang@zjnu.edu.cn (X.-Y. Wang), fangjch.syky@sinopec.com (J.-C. Fang).

further promoting the development of this method (Lan et al., 2019; Zhang et al., 2022).

Asphaltenes, with their complex structures and the presence of heteroatoms, play a crucial role in determining the viscosity of heavy oil (Wu et al., 2024; Yuan et al., 2023). Different forms of heteroatom-containing asphaltenes can give rise to diverse aggregation behaviors and intermolecular interactions within the heavy-oil system. For example, the self-aggregation of asphaltenes, which is frequently influenced by the type and distribution of heteroatoms, can directly affect the flow properties of heavy oil. The presence of heteroatoms (N, O, S) and trace metal ions (e.g., vanadium (V), iron (Fe), and nickel (Ni)) in heavy components has been demonstrated to not only elevate viscosity but also causes a decline in quality (Gao et al., 2013; Rahmati, 2021). Besides heteroatom species, the structural morphology of asphaltene may also affect its aggregation morphology and, consequently, the viscosity effect of heavy oil (Kuznicki et al., 2008; Mikami et al., 2013). However, the specific details of how different morphologies (such as linear and island structures) influence the viscosity characteristics of asphaltene remain to be elucidated (Zhu et al., 2024). Identifying the specific heteroatom-asphaltene forms that contribute most to high viscosity enables the development of more targeted in-situ viscosity-reduction strategies. This may involve the design of new chemical additives or adjusting extraction conditions to disrupt the aggregation of high-viscosity-causing

In recent years, experimental and simulation studies have clarified NOS heteroatom asphaltene's influence on heavy oil's viscosity from the self-assembly perspective (Fang et al., 2024; Gao et al., 2014; Wang et al., 2021; Yuan et al., 2023). These studies mainly focus on a single medium system or adopt a single asphaltene structure (Ahmadi and Chen, 2023; Bai et al., 2019; Fang et al., 2024; Liu et al., 2024; Tazikeh et al., 2022), but asphaltenes also possess exposed areas to resins and other components, which may introduce stronger intermolecular friction under shearing (Zhang et al., 2024). Only considering the aggregation mechanism of asphaltene cannot reflect the complexity of the environment in which asphaltene and heavy oil are located. In addition, studies have shown that asphaltenes with different aggregation characteristics have different effects in crude oil (Zhu et al., 2024), but have rarely studied the effects of heteroatoms on these different types of asphaltenes. The microscopic behaviors of different heteroatom forms and asphaltenes in real oil droplets vary (Silva et al., 2016). Studying the microscopic behaviors of different forms of heteroatom asphaltenes within real oil droplets can provide an in-depth understanding of their interactions with other components in the oil droplets, such as resins and light oil molecules (Yuan et al., 2023). Furthermore, it can clarify how heteroatom asphaltenes influence aggregation and how such an internal mechanism changes the microscopic structure and macroscopic viscosity of oil droplets (Fang et al., 2024).

Additionally, asphaltene deposition can lead to reservoir pore blockage and oil pipeline scaling (Alimohammadi et al., 2019). The adsorption and aggregation mechanism of heteroatom asphaltenes on the surface of reservoir minerals and the inner wall of pipelines is conducive to understanding the mechanism of asphaltene deposition, so that appropriate anti-scaling and descaling measures can be taken to ensure the normal exploitation of oil wells and the smoothness of oil pipelines (Alsehli et al., 2024; Sun et al., 2025). Studying the adsorption of heteroatom asphaltenes and formed oil droplets on the sludge surface can help better understand the migration and transformation laws of asphaltene, preventing soil and water pollution caused by the adsorption and desorption of asphaltene (Li et al., 2024; Yang et al., 2023). Thus, the adsorption properties of different forms of heteroatom

asphaltene and its oil droplets on these solid surfaces are also another focus of this study.

Based on the above concerns, we selected two asphaltenes with distinct heteroatoms and aggregation characteristics, and compared them with non-heteroatom asphaltenes using molecular dynamics (MD) simulation. We established multiple systems, including an asphaltene self-assembly system, asphaltene-solid surface system, and oil-in-water and oil-water-solid systems, to comprehensively explore the effects of heteroatoms and asphaltene morphology on aggregation and adsorption mechanisms. This research contributes to a better understanding of the heavy-oil microstructure, helps to a deeper understanding of the heavy-oil viscosity and oil-solid mixing process, and provides a solid foundation for the development of new viscosity reducers, the improvement of heavy-oil recovery, and the optimization of processing procedures.

2. Simulation methods

All the initial systems construction, MD simulation, and output analysis are performed by the Gromacs 2019 software package (Abraham et al., 2015). The force field of crude oil and silica molecules was GROMOS 54a7 force field parameters (Schmid et al., 2011), which were generated from the ATB (Automated Topology Builder) web server (Stroet et al., 2018). The main atom parameter information is given in Table S1 of the Supporting Information. The GROMOS 54a7 force field is a united-atom force field optimized for biomolecular and organic systems, with explicit parameterization for hydrocarbons, heteroatoms (e.g., S, N, O), and condensed-phase properties, and performs well in the interface system of oil droplet (Ji et al., 2020; Ma et al., 2023). Electrostatic potential (ESP) and weak interaction analysis are carried out by the wave function analysis software Multiwfn 3.8 (Lu and Chen, 2012), and VMD software is used for visualization (Humphrey et al., 1996).

2.1. Simulation models

The composition of heavy oil is complicated, especially the heavy components such as asphaltenes. In this work, four different continental asphaltene molecules were selected, including y-lin-PA3, n-lin-PA3, y-isl-Aspa, and n-isl-Aspa. PA3 is proposed based on atomic force microscope (AFM) measurements and scanning tunneling microscope (STM) orbitals images (Bai et al., 2019), which have long side chains connected to the core of PA3, just like a line (Schuler et al., 2015), named y-lin-PA3. Another kind of asphaltene is Aspa, which is based on atomic force microscopy characterization of continental-type asphaltene structure, just like an island (Guan et al., 2019), named y-isl-Aspa. To explore the influence of heteroatoms on asphaltene and oil droplet behavior, the heteroatom in y-lin-PA3 and y-isl-Aspa is replaced by a C atom, forming n-lin-PA3 and n-isl-Aspa, to represent non-heteroatom PA3 and Aspa, respectively (Fig. S1). A fully hydroxylated silica plate was constructed, and the intrinsic wetting characteristics of reservoir rocks were simulated at the atomic level by surface hydroxyl functionalization (Table S2). Both experimental and simulation results confirm the reliability of this model.

To compare the effects of heteroatoms and different asphaltenes on the properties of heavy oil, four different media models were established to simulate the micro-behavior of asphaltenes to real heavy oil droplets (Fang et al., 2024). Take the y-lin-PA3 asphaltene systems as an example:

(1) Only asphaltenes (A): 20 asphaltenes (only one kind) were added to a $10 \times 10 \times 10 \text{ nm}^3$ cuboid to study the self-assembly mechanism of asphaltenes. In these systems, the

- y-lin-PA3 system and the y-isl-Aspa system with heteroatoms were named as y-lin-A and y-isl-A, respectively. The control group without heteroatoms was named as n-lin-A and n-isl-A, respectively (system (1) in Fig. S2).
- (2) Only asphaltenes and silica surface (A/S): 50 asphaltenes (only one kind) are placed in a 10 × 10 × 10 nm³ box, with a solid silica size of 10 × 10 × 1.5 nm³, located below the box. This system is built to simulate the adsorption mechanism of asphaltene on the solid surface. The system model including y-lin-PA3 molecules is named as y-lin-A/S, and its control group is named as n-lin-A/S. The y-isl-Aspa molecules system and its control group follow the same rules (system (2) in Fig. S2).
- (3) Oil-in-water interface system (O/W): 10 asphaltenes (only one kind) (Fig. 1(a)), 47 resins (Fig. 1(b)), and 319 light oil molecules (Fig. S4), with the concentrations ratio of asphaltenes:resin:light oil = 14%:25%:61% (Fig. 1(c)) (Zhang et al., 2022), were put into a 10 × 10 × 10 nm³ box to simulate the actual heavy oil droplet. After the 50 ns NPT simulation, water molecules were added to construct the oil-in-water system. The system model containing y-lin-PA3 asphaltene molecules is named as y-lin-O/W, and its control group was named n-lin-O/W. The y-isl-Aspa and n-isl-Aspa asphaltene systems follow the same rules, the control group is shown in Fig. S3 (system (3) in Fig. S2).
- (4) Oil/water-silica surface system (O/W/S): based on equilibrated systems of (3) y-O/W and n-O/W, a silica slab was added at the bottom of the box to explore the influence of heteroatom asphaltenes on the interaction of heavy crude oil droplets and silica surface, and the new systems were named as y-O/W/S and n-O/W/S, respectively (system (4) in Fig. S2).

2.2. Simulation details

Before NPT/NVT simulation, all systems underwent energy minimization and had their maximum energy below 100 kJ/mol.

The schematic diagram of the simulation process is shown in Fig. S2. For the asphaltenes system (A) and asphaltene/silica (A/S) surface system, the 50 ns NVT simulation was performed. A 50 ns NPT simulation was carried out for the mixture of asphaltene, resin, and light oil to form the oil droplet. The formed oil droplets are put into a $10 \times 10 \times 10 \text{ nm}^3$ cubic box, and water is added into the gap of the box to develop an oil-in-water system (O/W). A further 50 NVT equilibrium is carried out for this system. Based on the stable O/W systems, the $10 \times 10 \times 1.5 \text{ nm}^3$ silica slab was inserted into the bottom of the box to build the oil/water-silica surface system (O/W/S), and a longer simulation time (150 ns) was carried out for this system to capture the dynamic equilibrium and interfacial recombination process.

The water model used in this work is the SPC/E model. The simulations are conducted using a time step of 2 fs, and periodic boundary conditions (PBC) are applied in all directions (*x*, *y*, *z*) to maintain system continuity, minimize edge artifacts, and simulate an effectively infinite bulk environment. To maintain a constant temperature of 298.15 K, the v-rescale thermostat (Bussi et al., 2007) was used. Similarly, the Parrinello-Rahman method (Parrinello and Rahman, 1981) was employed to keep the system pressure at 1 atm. The LINCS algorithm (Hess et al., 1997) was utilized to constrain bonds between H-atoms. Particle mesh Ewald (PME) code (Darden et al., 1993) was used in the MD process, while the cut-off was used to handle electrostatic and van der Waals (VdW) interaction energy with a distance of 1.4 nm (Darden et al., 1993).

3. Results and discussions

The root-mean-square deviation (RMSD) can reflect the deviation of the oil molecule from its initial position as the simulation progresses, which is employed to prove that the target system reaches equilibrium. As shown in Fig. S5, the RMSD curve fluctuated in a small range after 30 ns, all systems reached an equilibrium state within the 50 ns simulation time.

y-lin-PA3 y-isl-Aspa (b) CH ₃ CH ₃	
(b) CH ₃ CH ₃	
H_3C CH_3 $Resin 1$ $Resin 2$ H_3C H_3C H_3C $Resin 3$	
$\begin{array}{cccccccccccccccccccccccccccccccccccc$	

(c) Crude oil component		Number
Asphaltene	y-lin-PA3 or y-isl-Aspa	10
Resin	Resin 1	8
	Resin 2	8
	Resin 3	7
	Resin 4	8
	Resin 5	8
	Resin 6	8
Light oil	Benzene	20
	Toluene	52
	Cyclohexane	33
	Cycloheptane	52
	Nonane	60
	Octane	50
	Heptane	44
	Hexane	48

Fig. 1. The (a) heteroatom asphaltene and (b) resin structural formulas used in the simulations of the heteroatom oil droplets system and (c) the molecule composition of heteroatom oil droplets.

The electrostatic potential (ESP) (Zhang and Lu, 2021) of every asphaltene molecule is first analyzed, as shown in Fig. 2. The ESP was calculated and analyzed at the SMD/M062X//6-311++G(3df, 2p) level (Yuan et al., 2023) by Gaussian 16 (Frisch et al., 2016) and Multiwfn software. In the four asphaltene models, the positive ESP region is distributed on the side chain, while the negative ESP region is mainly located on the aromatic ring. Due to the long sidechain of linear PA3, it has a larger positive area and a smaller negative area. The difference between positive and negative areas of y-lin-PA3, n-lin-PA3 is also larger than y-isl-Aspa, n-isl-Aspa (Fig. 2). The existence of heteroatoms will increase the negative electrostatic potential area on the asphaltene surface, thus narrowing the difference between the positive and negative potentials on the asphaltene surface. This is because heteroatoms usually have high electronegativity (N, O atoms) or lone pair electrons (S atom), forming local negative centers in the molecular structure. Although the area corresponding to the maximum and minimum value of ESP is small, the difference between the maximum and minimum of heteroatom asphaltene is larger than that of non-heteroatom asphaltene.

3.1. The self-aggregation behavior of asphaltenes

Self-aggregation of asphaltenes has always been the primary concern (Fang et al., 2024; Kuznicki et al., 2008). To detail analysis of the self-aggregation morphology of different asphaltene (heteroatoms and non-heteroatoms, linear PA3, and island Aspa), the radial distribution function (RDF) on each system was first carried out, as shown in Fig. 3. The first peak of the RDF line represents the face-to-face adsorption structure between the asphaltene molecules and the other peak represents the edge-to-face adsorption or other (side-to-side, etc.) adsorption structure, this is also in line with the previous studies (Yuan et al., 2023). The first aggregation layer of the face-to-face structure of the isl-Aspa molecule is larger than that of lin-PA3, but the aggregation distance of lin-PA3 is shorter than y/n-isl-Aspa. The central polycyclic aromatic

hydrocarbon of the Aspa molecule has a large structural area, which is more conducive to face-to-face adsorption (Yuan et al., 2023). PA3 molecule has a less face-to-face aggregation configuration and is inclined to edge-to-face adsorption. This is because of the complex side-chain in PA3, facilitating them to intertwine during asphaltene aggregation, which prevents them from forming a single face-to-face adsorption structure. Moreover, the RDF line of lin-PA3 has more peaks, indicating that lin-PA3 tends to be a multi-layer face-to-face or edge-to-face aggregation structure (especially heteroatom asphaltene).

In detail, the lin-PA3 has a closer aggregation distance compared to isl-Aspa. This may be attributed to a larger ESP difference between positive and negative areas of lin-PA3. The complementary arrangement of positive and negative potential regions (such as face-to-face or face-to-edge) compresses the molecular spacing. However, v/n-isl-Aspa has a large aromatic ring aggregate, and the π - π interaction of aromatic rings promotes the asphaltene face-to-face aggregation, while the negative electrostatic potentials on the surface of large aromatic rings repel each other. Moreover, the total face-to-face aggravate total peak value of y-lin-PA3 is larger than n-lin-PA3, and the formation distance of the face-to-face structure of the former (0.281 nm) is shorter than the latter (0.441 nm) (Fig. 3(a) and (b)). The existence of heteroatoms in PA3 asphaltene makes this asphaltene self-assemble tightly, which is related to the larger difference between the maximum and minimum ESP value of y-lin-PA3 than n-lin-PA3. The v-isl-Aspa and n-isl-Aspa had similar formation trends for the face-to-face and edge-to-face structures (Fig. 3(c) and (d)). The large \triangle ESP in heteroatom asphaltenes induces the enhancement of intermolecular dipole-dipole interaction and enhances the electrostatic attraction between molecules, and promotes the formation of tight stacking of molecules faster.

To determine the self-assembly stability of asphaltene, the average interaction energy of the face-to-face and the edge-to-face structures of two asphaltene molecules was calculated (Fig. 4). The asphaltene interaction mainly depends on Van der Waals

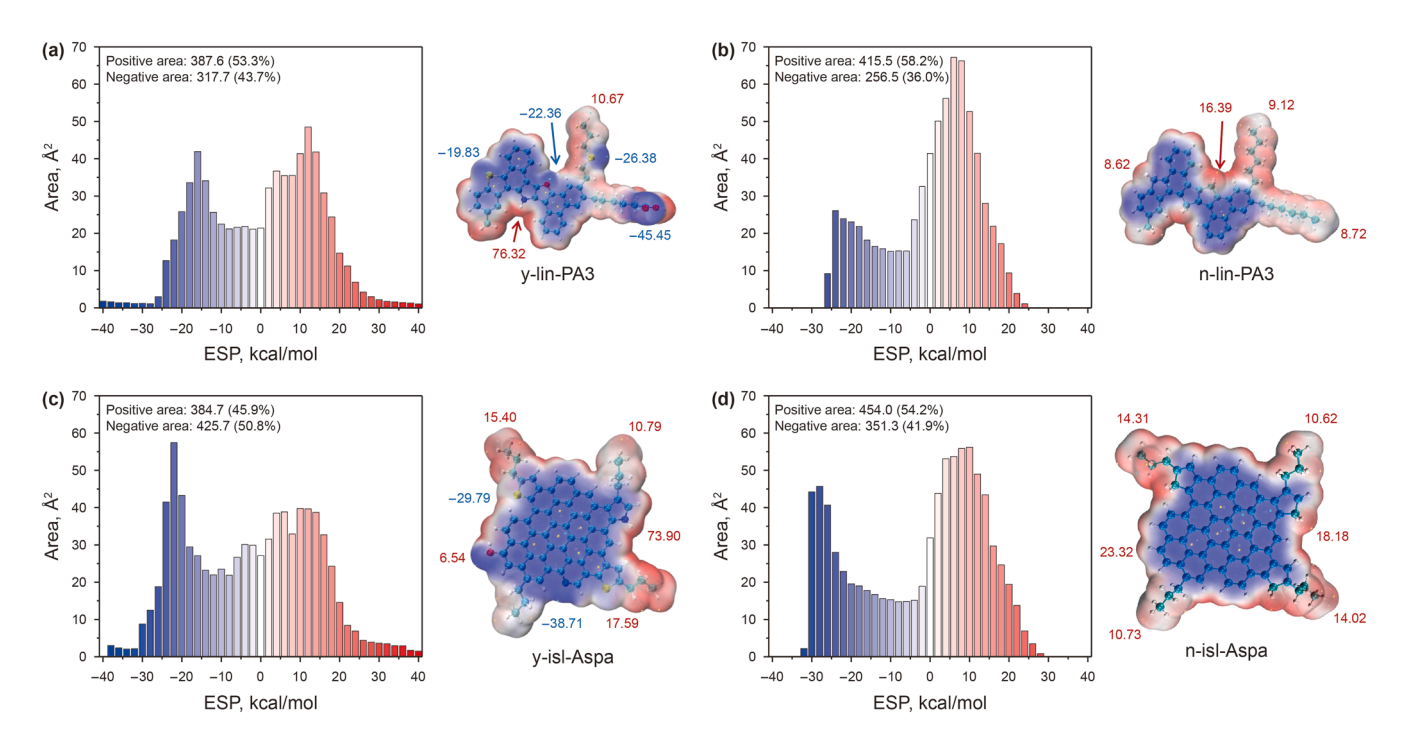


Fig. 2. The electrostatic potential (ESP) value distribution (right) and the detailed distribution regions on the asphaltene surface (left) for (a) y-lin-PA3, (b) n-lin-PA3, (c) y-isl-Aspa, and (d) n-isl-Aspa molecules.

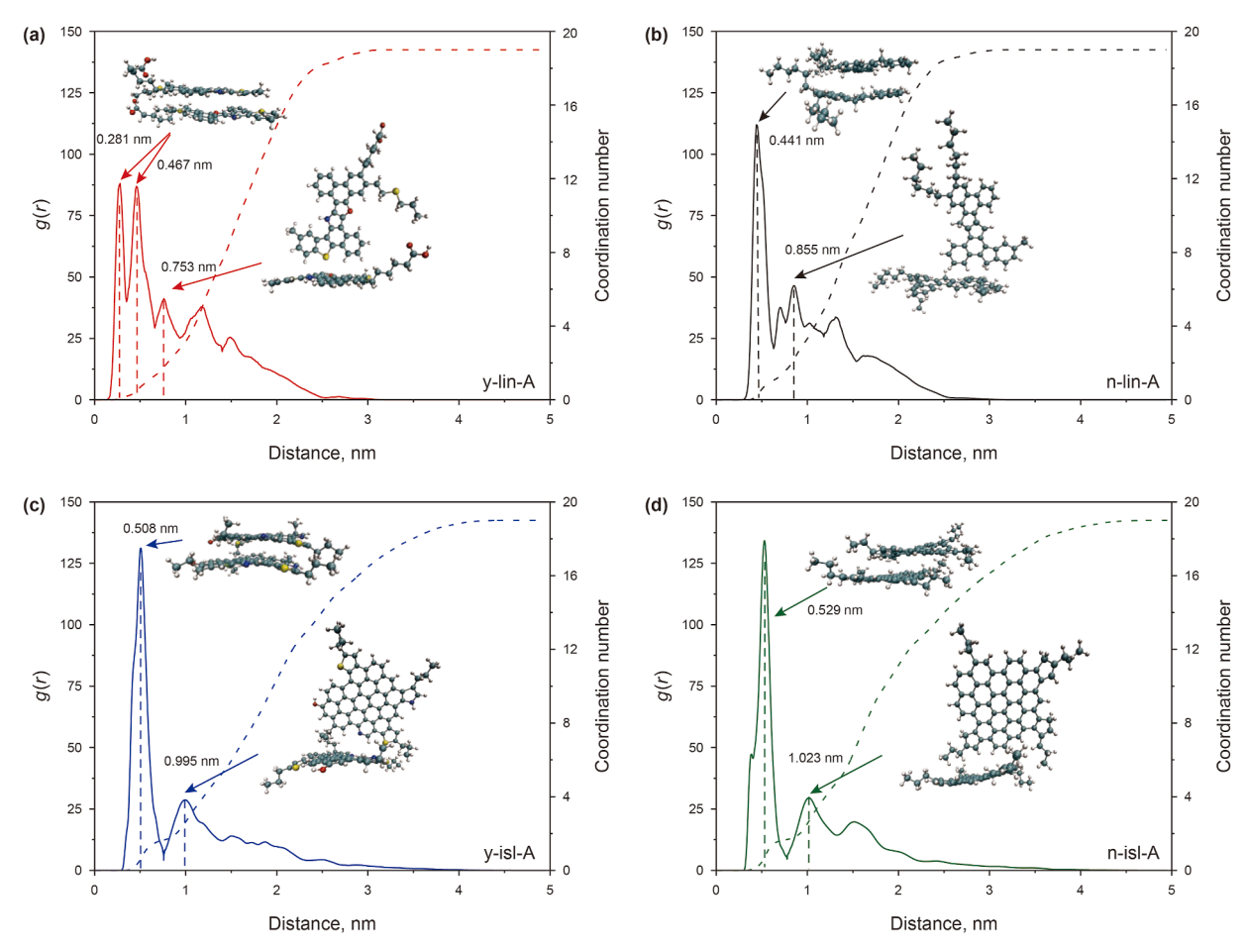


Fig. 3. The radial distribution function (RDF) between asphaltene and asphaltene for **(a)** y-lin-A, **(b)** n-lin-A, **(c)** y-isl-A, and **(d)** n-isl-A systems. The solid line and dotted line represent RDF (g(r)) and coordination number (N), respectively.

interaction energy, which is verified by the green iso-surface between two asphaltene molecules (Fig. 5). The total interaction energy of island Aspa is always larger than linear PA3 for both the face-to-face and the edge-to-face self-assembly structures. RDF and interaction energy show that the strong interaction energy between island Aspa may not be due to its closer packing, but to its greater atomic number and benzene ring structure than that of PA3. This result is in line with the laboratory viewpoint that asphaltenes with more aromatic ring structures have a stronger self-aggregate trend (Horeh et al., 2023). Taking the face-to-face nlin-A and n-isl-A as examples, the total interaction energy of n-isl-A is 89.93 kJ/mol larger than n-lin-A (Fig. S6). Generally, the selfassembly energy of heteroatom asphaltenes is larger than that of non-heteroatom asphaltenes. However, the edge-to-face energy and total energy of n-lin-A is slightly larger than y-lin-A (Fig. 4(c)and Fig. S6(a), which may be due to a larger VdW weak interaction of y-lin-A than n-lin-A at the same iso-surface value (Fig. 5(b)).

3.2. The adsorption behavior of asphaltene on silica surfaces

Due to the deposition phenomenon of heavy oil on the surface of rocks and equipment in mining and processing, and the remediation of oil-contaminated soil, the adsorption of asphaltene on the solid surface model is also simulated. The molecular structure of these substrates is mainly silicon-oxygen tetrahedron and aluminum-oxygen octahedron, and the elements of oxygen and silicon account for the largest proportion, accounting for 49% and

33% respectively. As a result, SiO_2 is expected to be the best model for these adsorption substrates (Awad et al., 2019; Zhao et al., 2022).

The snapshots of four A/S systems with simulation times were intercepted, as shown in Fig. S7. Asphaltene molecules near the silica surface tend to be directly adsorbed on the silica surface, while the asphaltene molecules far away from the silica surface tend to self-aggregate and then be adsorbed on the solid surface. Thus, both single molecule adsorption and aggregation adsorption exist on the surface of silica, and aggregation adsorption is the dominant adsorption form, which is also consistent with the result by Mendoza et al. that asphaltene interacts with silica rock sample by the multi-layer adsorption method at high concentration (Mendoza et al., 2009). The spatial distribution function (SDF) is also calculated to investigate the distribution of asphaltenes on the solid surface, as shown in Fig. 6. The solvent-accessible surface area (SASA) of the asphaltenes-solid surface adsorption system is carried out to quantify the adsorption situation. The SASA of the solid surface for the heteroatom asphaltene systems is larger than the non-heteroatom asphaltene systems, indicating a higher aggregation degree of heteroatom asphaltene. This also follows the loose SDF of n-lin-A/S and n-isl-A/S compared to y-lin-A/S and yisl-A/S. In addition, the SASA of the Aspa asphaltene system is smaller than that of the PA3 system in both the heteroatom and non-heteroatom systems, which indicates that the distribution area of Aspa on the surface of silica is larger than that of PA3. These simulated microscopic results further verify the rationality of the

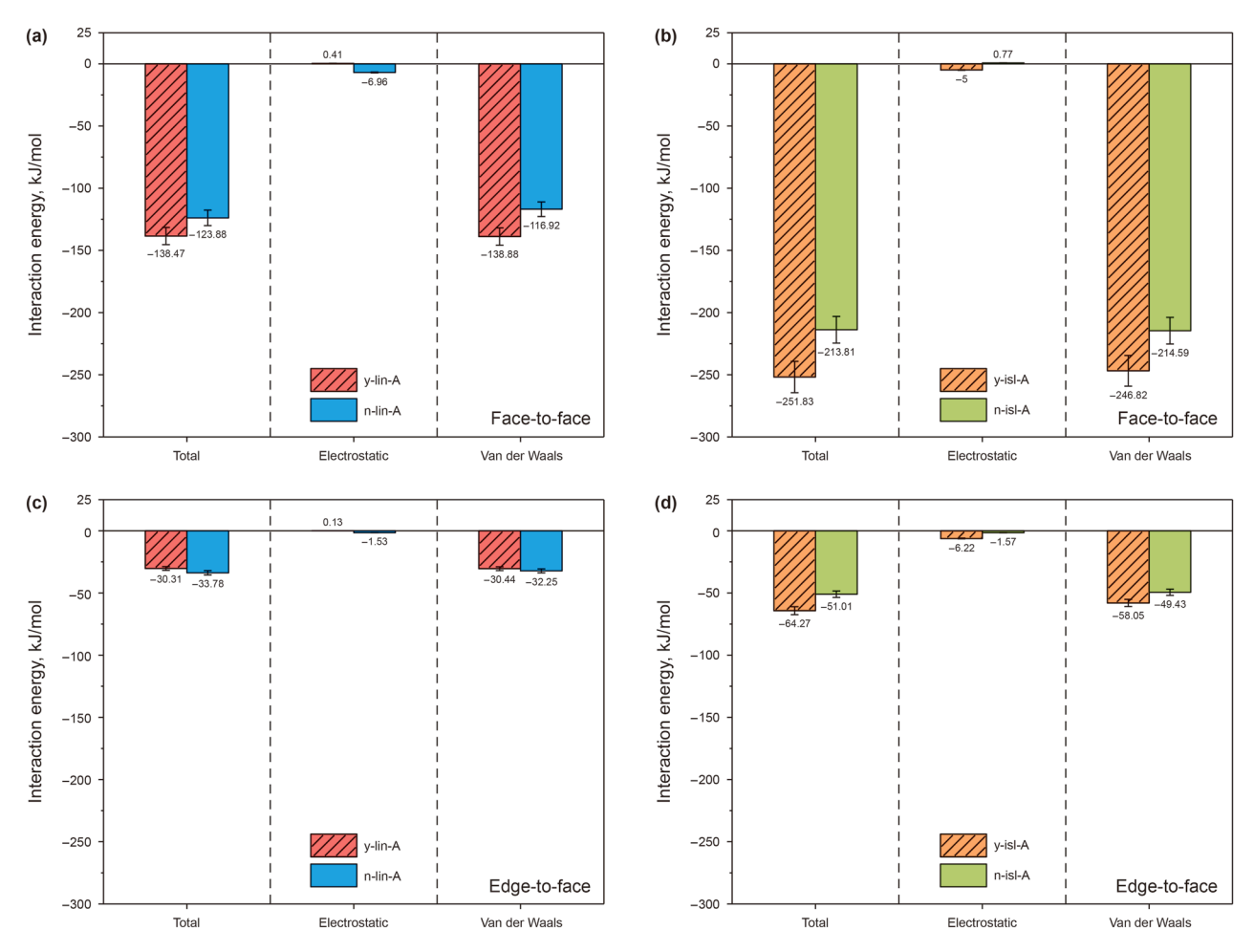


Fig. 4. Energy decomposition analysis of the interaction of (a) the face-to-face of PA3 molecules, (b) the face-to-face of Aspa molecules, (c) the edge-to-face of PA3 molecules, and (d) the edge-to-face of Aspa molecules in A system.

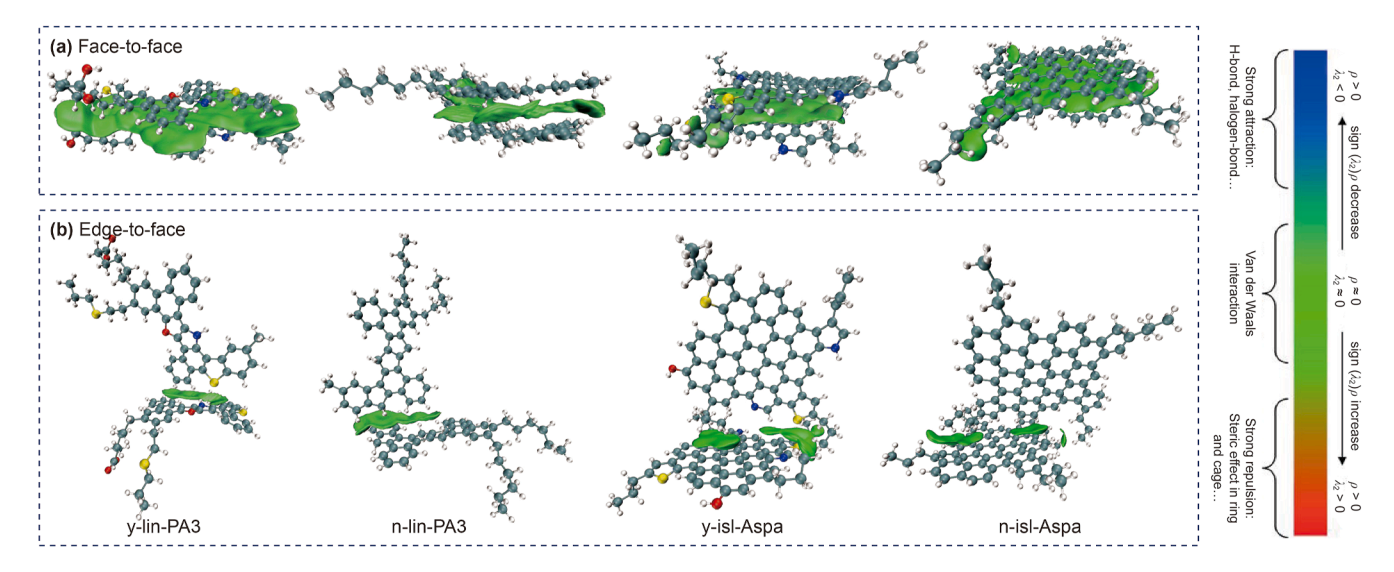


Fig. 5. The weak interaction of the (a) face-to-face adsorption and (b) edge-to-face adsorption between the asphaltene-based IGMH model.

speculation that heteroatom content and asphaltene configuration will affect its adsorption on the rock surface (González et al., 2007).

The further energy result (Fig. S8) shows that the adsorption energy of asphaltene molecules on the silica surface is dominated by VdW interaction energy. The total adsorption energy of

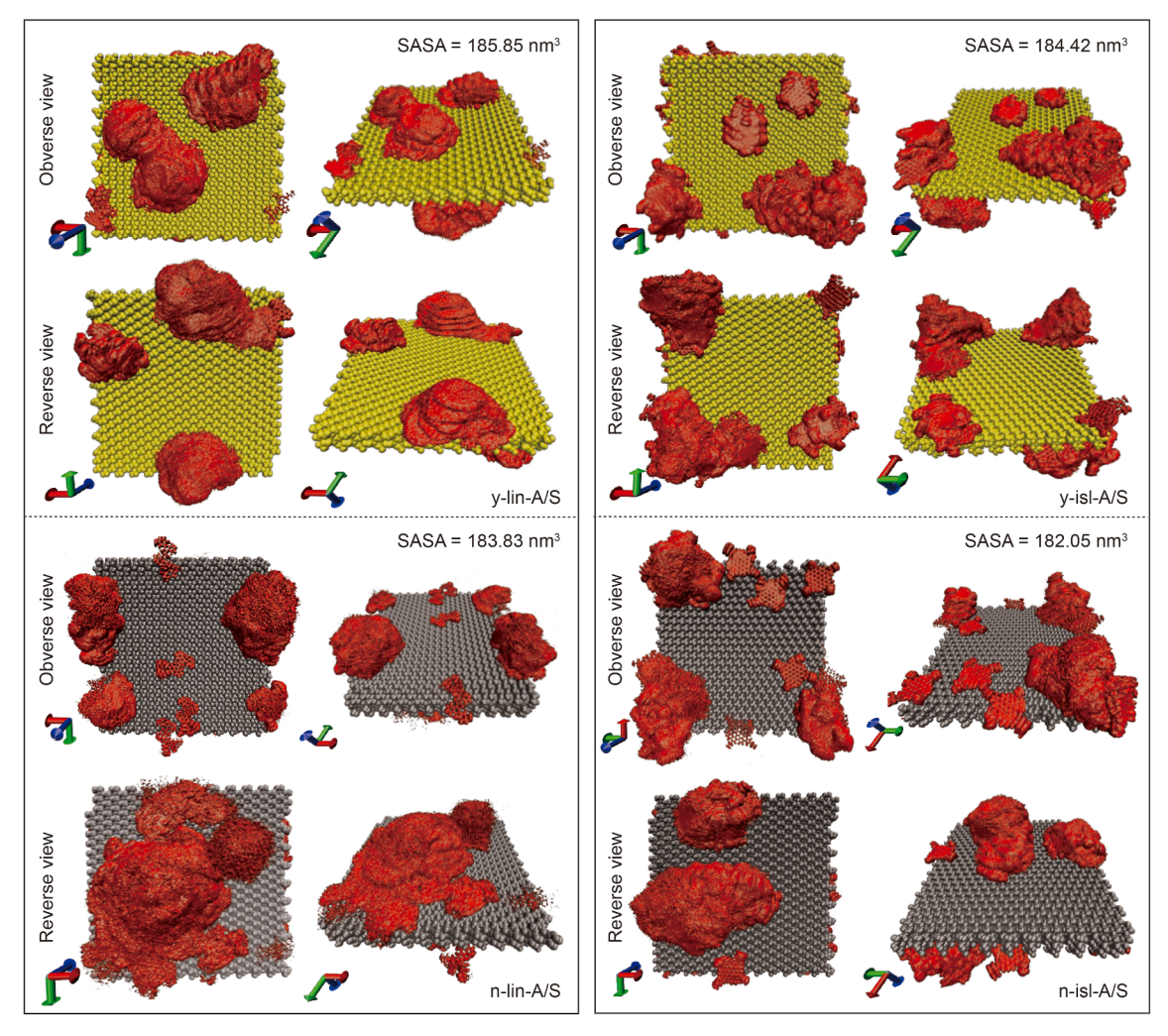


Fig. 6. The spatial distribution function (SDF) of four asphaltenes on the solid surface and the corresponding SASA of the solid surface in A/S systems.

heteroatom asphaltene is also larger than non-heteroatom asphaltene, which is consistent with previous theoretical and experimental research results (Bai et al., 2019). In addition, the total adsorption energy of the island Asp is larger than linear PA3. The large area and tight adsorption of heteroatom asphaltene, especially island heteroatom asphaltene (y-isl-A/S), on the surface of silica may make it difficult to peel off the mineral surface.

To understand the aggregation configuration of asphaltene on the silica surface, the g(r) of the center of molecule (COM) of asphaltene concerning the silica surface was calculated, as shown in Fig. 7. Both lin-PA3 and isl-Aspa interact with the solid surface through tiled and tilted adsorption. The heteroatoms and nonheteroatoms systems have similar adsorption distances and peak values on the first tiled adsorption layer on the solid surface. However, the first g(r) peak of isl-Aspa is larger than lin-PA3, which indicates that island asphaltene has a higher tiled adsorption trend on the solid surface than linear asphaltene. Notably, there are multiple adsorption peaks in the g(r) line of the four systems (especially lin-PA3), indicating that asphaltene is adsorbed on the surface of silica in multiple layers. Among them, inear asphaltene has long branched chain and high molecular flexibility, which can adjust the conformation during adsorption and form multi-layer aggregation more easily. This is also in line with the laboratory results and SDF/SASA results (Mendoza et al., 2009).

3.3. The behavior of heteroatom/non-heteroatom asphaltene in the oil/water system

Based on asphaltene's self-assembly and adsorption behavior, the influence of heteroatom asphaltene on the real oil droplet system deserves concern.

RDF is employed to demonstrate the distribution of various components of oil droplets (Fig. 8). The final snapshots of oil droplets in the O/W systems are shown in Fig. 8(a). All asphaltene and resin molecules are distributed at the oil-water interface (Figs. S9 and S10). Face-to-face self-aggregation is the main form of asphaltene accumulation at the oil-water interface, and the formation trend of heteroatom asphaltenes is larger than the nonheteroatom system (Fig. 8(b)). For both the lin-PA3 and isl-Aspa systems, the resin peak intensity around heteroatom asphaltenes is larger than the non-heteroatom asphaltenes (Fig. 8(c)), which suggests heteroatom asphaltenes have stronger interaction trend with resin. Notably, the heteroatom in the PA3 structure may have an obvious effect that is different from the corresponding nonheteroatom asphaltene, which can be verified by the larger difference in first peak intensity between y-lin-PA3 and n-lin-PA3. The peak intensity between asphaltene and light oil is weak, and the peak intensity of heteroatom asphaltene with light oil component is smaller than that of non-heteroatom asphaltene (Fig. 8(d)).

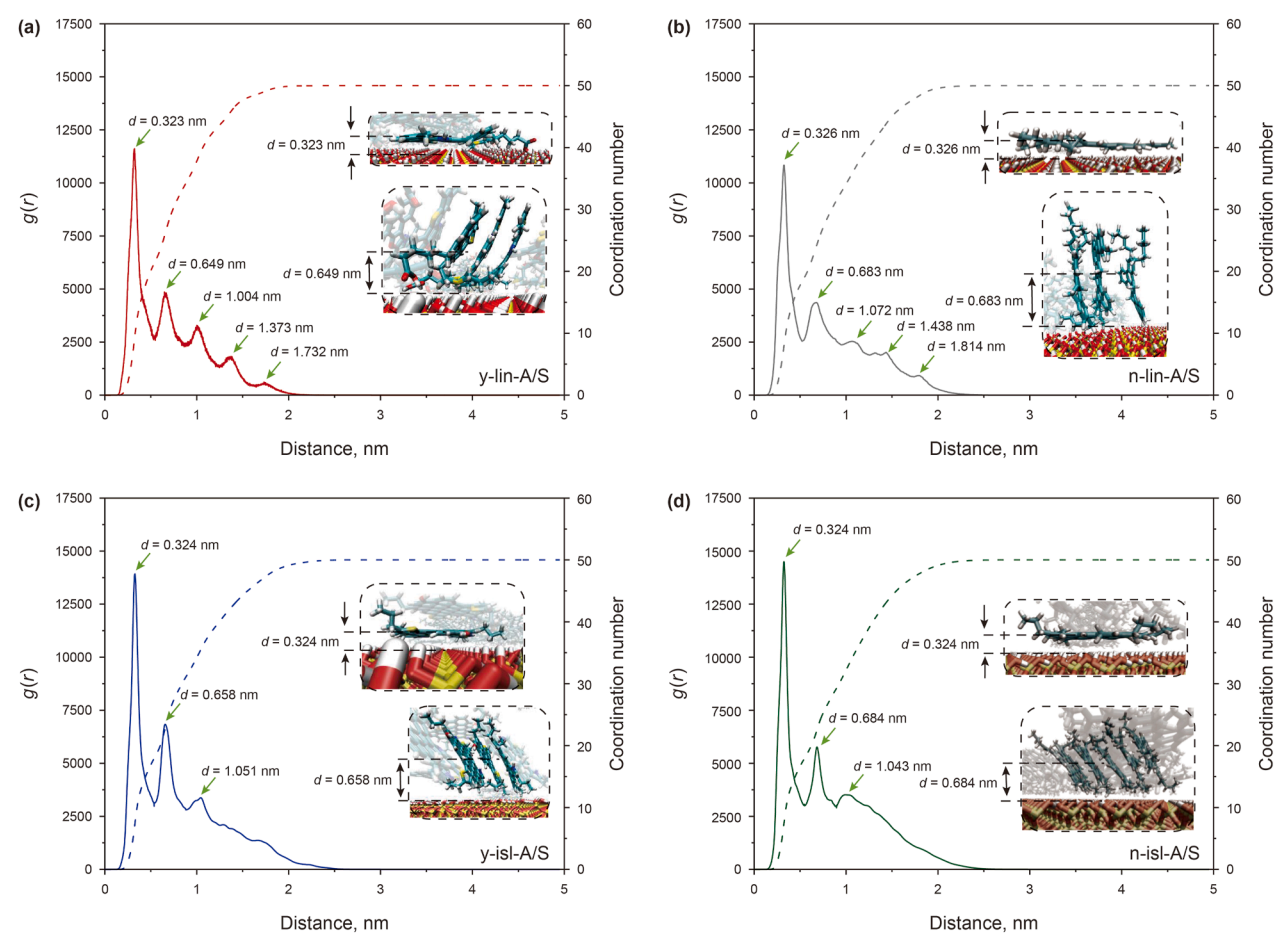


Fig. 7. The radial distribution function (RDF) between the COM of asphaltene and the silica surface in the (a) y-lin-A/S system, (b) n-lin-A/S system, (c) y-isl-A/S system, and (d) n-isl-A/S system. The solid line represents g(r), and the dotted line represents the coordination number (N).

Fig. S11 tests the interaction energy between asphaltene, resin, and light oil. For the lin-PA3 system (Fig. S11(a)-(b)), compared with the energy difference of self-aggregation (system A), the interaction energy between heteroatom asphaltenes in oil droplets is very close to that of non-heteroatom asphaltenes, which is due to the strong connection between heteroatom asphaltene and other components in real oil droplets. The interaction energy of heteroatom lin-PA3 with resin and light oil components is 317 kJ/ mol and 266 kJ/mol greater than that of non-heteroatom lin-PA3, respectively. The heteroatom lin-PA3 has obvious face-to-face aggregation, while the non-heteroatom lin-PA3 is dispersed at the oil-water interface, which makes the contact area between the non-heteroatom lin-PA3 and water larger, so the interaction between the non-heteroatom lin-PA3 and water is greater than that of the heteroatom lin-PA3. For the isl-Aspa system (Fig. S11(c)-(d)), the interaction energy between heteroatoms is also lower than that of the self-aggregation system. Although the interaction energy of heteroatom asphaltene and light oil is lower than that of the non-heteroatom system, heteroatom asphaltene shows strong interaction energy with itself and resins. The interaction between heteroatom isl-Aspa asphaltene and water is larger than nonheteroatom isl-Aspa asphaltene, which is different from lin-PA3.

The diffusion coefficients of resin molecules, light oil molecules, and all crude oil molecules and viscosity of oil droplets are also calculated to reflect the influence of asphaltene on the oil droplet component, as shown in Fig. 9. Whether it is PA3 or Aspa, the diffusion coefficient of resin, light oil components and whole

oil droplets in the heteroatom system is lower than that in the non-heteroatom system, and this suggests that the existence of heteroatoms reduces the fluidity of other components and whole oil droplets (Fig. 9(a)-(c)). The viscosity of the four oil droplet systems also takes the order of y-isl-O/W > n-isl-O/W > y-lin-O/ W > n-lin-O/W. The viscosity of island heteroatom asphaltene oil droplets is higher than that of linear heteroatom asphaltene oil droplets. The experimental conclusion that asphaltene configuration may have an important influence on its aggregation structure, thus affecting the surface tension of aggregates formed by heavy oil components, is further verified (Ghatee and Shabih, 2017). However, it is worth noting that the difference in diffusion coefficient between y-isl-PA3 and n-isl-PA3 systems is greater than that between y-isl-Aspa and n-isl-Aspa systems, indicating that the presence of heteroatoms in linear PA3 asphaltenes has a more obvious effect on the viscosity of heavy oil, which is well proved the viscosity difference results in Fig. 9(d).

3.4. The influence of solid surface on oil droplet behavior

The behavior of heteroatom and non-heteroatom oil droplets on the silica mineral surface is further understood. Fig. 10 shows the change in the center of mass (COM) distance between oil droplets and mineral surface in y-O/W/S and n-O/W/S systems with the 150 ns simulation time. The COM distance of the heteroatom oil droplet changes from 4.96 to 2.26 nm, while the COM distance of the non-heteroatom oil droplet changes from 4.85 to

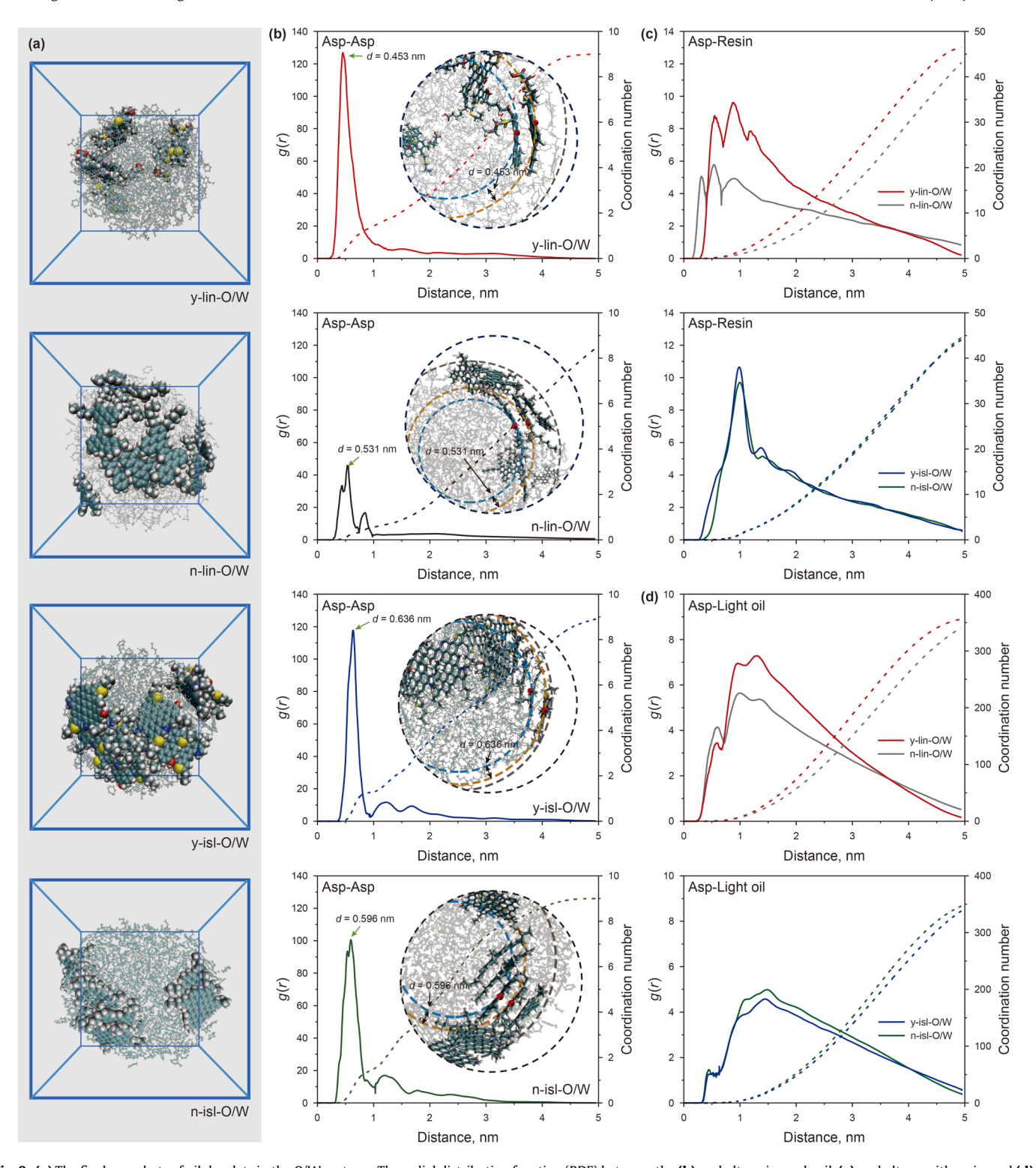


Fig. 8. (a) The final snapshots of oil droplets in the O/W systems. The radial distribution function (RDF) between the (b) asphaltene in crude oil, (c) asphaltene with resin, and (d) asphaltene with light oil. The asphaltene molecules are shown as a spherical model; the remaining molecules are other crude oil molecules, and the water molecules are ignored.

2.27 nm. The oil droplets in the presence of heteroatoms move 0.12 nm more than those in the presence of non-heteroatom asphaltenes in the vertical direction (Fig. 10(a) and (b)). Though the COM distance between heteroatom/non-heteroatom oil droplets and non-heteroatom oil droplets is close after equilibrium, the interaction energy between heteroatom oil droplets and

the surface is 163.99 kJ/mol higher than that of non-heteroatom oil droplets.

Through the density distribution of oil droplet components (Fig. 10(c) and (d)) and the energy decomposition calculation between this component and the solid surface (Fig. 10(e)), it is found that rather than the interaction between heteroatom asphaltene

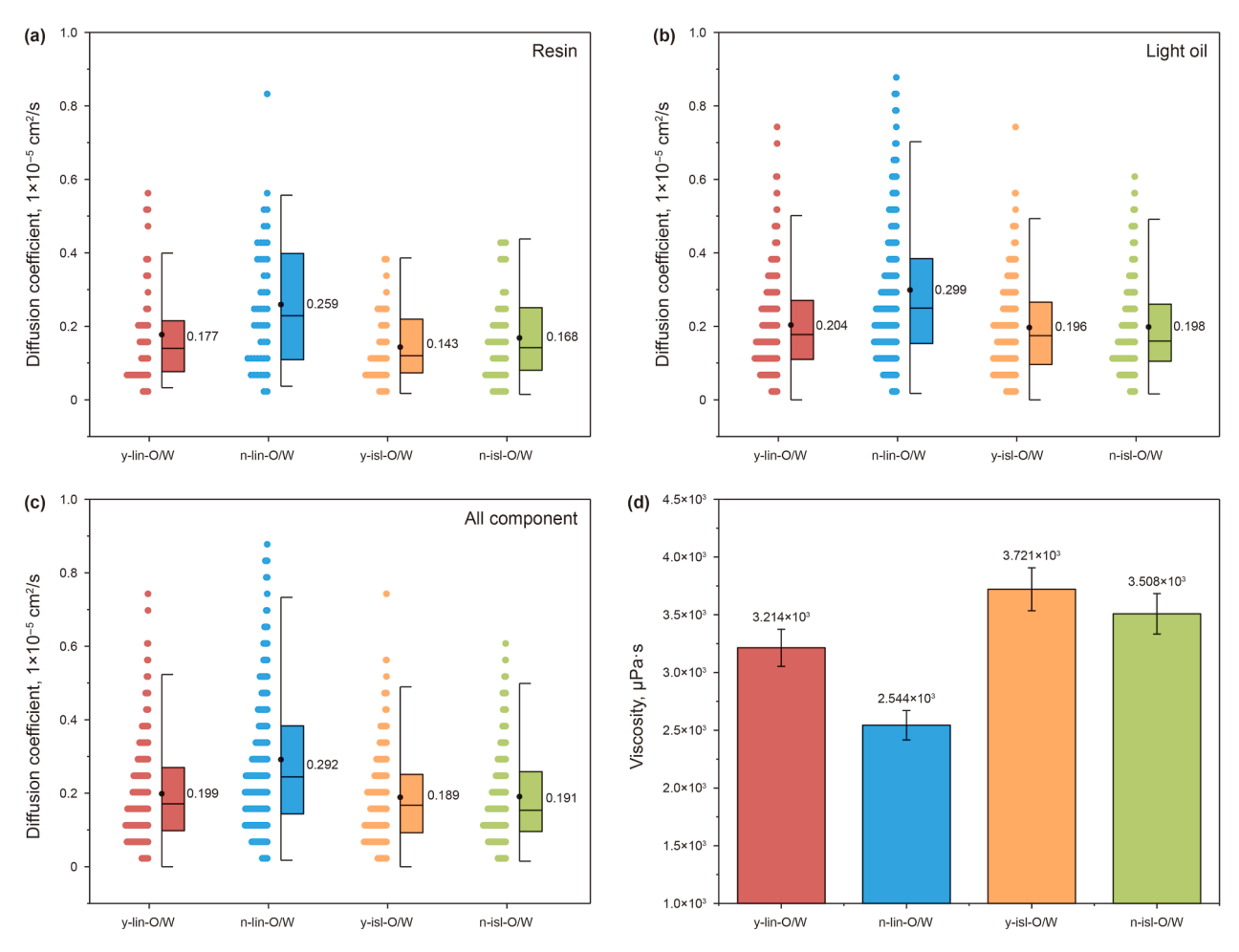


Fig. 9. The diffusion coefficients of (a) resin molecules, (b) light oil molecules, and (c) all crude oil molecules in O/W systems; (d) the viscosity of oil droplets in O/W systems.

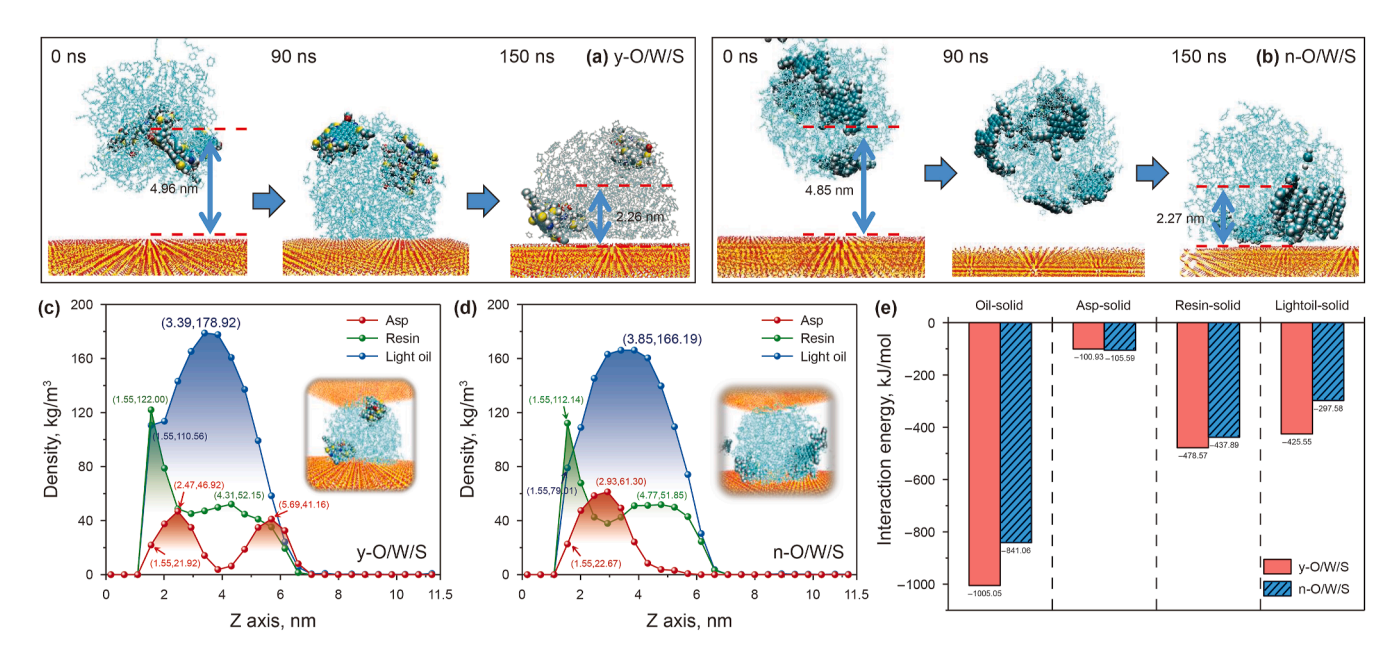


Fig. 10. Snapshot diagram of (a) heteroatom and (b) non-heteroatom oil droplet adsorption process, (c) and (d) density of crude oil components vary with Z-axis, and (e) interaction energy between oil droplet components and solid surface.

and the solid surface, the stronger interaction of heteroatom oil droplets and the surface is due to the stronger interaction energy between other components in heteroatom oil droplets, especially light oil components and the solid surface. The heteroatom asphaltene shows competitive adsorption with the light oil components on the solid surface, so only some heteroatom asphaltene is at the oil-solid interface, and some are far away from the surface. The highest density peak of light oil components corresponds to the valleys of asphaltene. These factors make the light oil components in heteroatom oil droplets more concentrated at the liquid-solid interface. The adsorption energy change of each component in the droplet on the solid surface is also calculated to support this result (Fig. S12). At the beginning of adsorption, the light oil component is first adsorbed on the silica. Then the resins begin to replace the part of light oil, with the increased adsorption energy of resins and decreased adsorption energy of light oil. At the late adsorption stage, asphaltene began to take the place of resin, and the adsorption energy of resin decreased, and the adsorption energy of light oil slightly increased (especially for the heteroatom oil-droplets system) and stabilized.

4. Conclusions

This study underscores the critical role of heteroatoms in modulating the aggregation and adsorption behaviors of asphaltenes, significantly impacting the viscosity and interaction dynamics of oil droplets with solid surfaces. These insights are pivotal for understanding and managing the challenges associated with heavy oil recovery and processing. The key findings are summarized as follows:

- (1) Linear heteroatom asphaltenes exhibit a multi-layered selfaggregation pattern, forming denser structures than island heteroatom asphaltenes. However, island heteroatom asphaltenes demonstrate stronger aggregation energy due to their higher benzene ring content and greater atomic number.
- (2) The adsorption energy of heteroatom asphaltene is 100.89 and 484.18 kJ/mol larger than that of non-heteroatom asphaltene, and the aggregation pile of the former is also larger than the latter, which indicates that the existence of heteroatoms makes asphaltene interact more strongly with the surface. The tight adsorption of heteroatom asphaltene makes it difficult to remove from mineral surfaces.
- (3) Linear heteroatom asphaltenes form multi-layered aggregates on solid surfaces, but island heteroatom asphaltenes show a more dispersed aggregation adsorption structure with a smaller solvent-accessible surface area. Moreover, the adsorption energy of island heteroatom asphaltene on the solid surface is larger than that of linear heteroatom asphaltene. Considering the strong self-aggregation and adsorption energy, island heteroatom asphaltene indicates stronger interaction with the silica surface.
- (4) Heteroatom asphaltenes form stronger interactions with resins within oil droplets, which reduces the diffusion capability of both the resins and the oil droplets, thereby decreasing overall fluidity. Although the presence of heteroatoms in linear asphaltenes has a more pronounced effect than island heteroatom asphaltenes on both the behavior of asphaltene and the viscosity of the oil droplets, the island heteroatom asphaltenes exhibit the strongest interaction energy with themselves and resins, leading to the most significant viscosity increase in oil droplets.
- (5) Heteroatom-containing oil droplets are found closer to solid surfaces and exhibit stronger interaction energies compared

to non-heteroatom oil droplets. This enhanced interaction is likely due to the influence of heteroatom asphaltenes on other components, particularly light oil fractions, facilitating the interaction of light oil fractions with the solid surface.

Our study focused on two representative asphaltene molecular structures (lin-PA3 and isl-Aspa) and their non-heteroatom counterparts. While this simplification allowed us to isolate the role of heteroatoms in asphaltene and oil droplets aggregation and adsorption, it does not fully capture the natural polydispersity of real asphaltene. A comprehensive understanding of the asphaltene behavior mediated by heteroatoms also depends on the influence of asphaltene polydispersity on aggregation and adsorption, and the adsorption mechanism of asphaltene and heavy oil is related to the temperature, pressure, and rock composition. The influence of these factors on heteroatom asphaltene effect needs to be further investigated.

CRediT authorship contribution statement

Guan-Dong Wang: Writing – original draft, Data curation, Software, Investigation, Writing – review & editing, Formal analysis. **Peng-Cheng Zou:** Supervision, Methodology, Investigation, Writing – original draft. **Si-Si Cheng:** Investigation, Formal analysis, Validation, Data curation, Methodology. **Yong Hu:** Resources, Project administration, Supervision, Software. **Xue-Yu Wang:** Methodology, Data curation, Investigation, Conceptualization, Writing – review & editing, Funding acquisition, Writing – original draft, Formal analysis. **Ji-Chao Fang:** Supervision, Methodology, Software, Funding acquisition, Resources, Visualization, Project administration.

Declaration of competing interest

The authors declare that they have no known competing financial interests or personal relationships that could have appeared to influence the work reported in this paper.

Acknowledgments

The work is supported financially by the National Natural Science Foundation of China (No. 52204069, No. 22306171), the Natural Science Foundation of Zhejiang Province (No. LQ24B070005), and the Jinhua Natural Science Foundation of China (2023–4–024).

Appendix A. Supplementary data

Supplementary data to this article can be found online at https://doi.org/10.1016/j.petsci.2025.07.025.

References

Abraham, M.J., Murtola, T., Schulz, R., et al., 2015. GROMACS: high performance molecular simulations through multi-level parallelism from laptops to supercomputers. SoftwareX 1, 19–25. https://doi.org/10.1016/j.softx.2015.06.001.

Ahmadi, M., Chen, Z., 2023. Molecular dynamics investigation of wettability alteration of quartz surface under thermal recovery processes. Molecules 28, 1162. https://doi.org/10.3390/molecules28031162.

Alimohammadi, S., Zendehboudi, S., James, L., 2019. A comprehensive review of asphaltene deposition in petroleum reservoirs: theory, challenges, and tips. Fuel 252, 753–791. https://doi.org/10.1016/j.fuel.2019.03.016.

Alsehli, M., Basem, A., jasim, D.J., et al., 2024. Insights into water-lubricated transport of heavy and extra-heavy oils: application of CFD, RSM, and metaheuristic optimized machine learning models. Fuel 374, 132431. https://doi. org/10.1016/j.fuel.2024.132431.

- Awad, A.M., Shaikh, S.M.R., Jalab, R., et al., 2019. Adsorption of organic pollutants by natural and modified clays: a comprehensive review. Sep. Purif. Technol. 228, 115719. https://doi.org/10.1016/j.seppur.2019.115719.
- Bai, Y., Sui, H., Liu, X., et al., 2019. Effects of the N, O, and S heteroatoms on the adsorption and desorption of asphaltenes on silica surface: a molecular dynamics simulation. Fuel 240, 252–261. https://doi.org/10.1016/j.fuel. 2018.11.135.
- Bera, A., Babadagli, T., 2015. Status of electromagnetic heating for enhanced heavy oil/bitumen recovery and future prospects: a review. Appl. Energy 151, 206–226. https://doi.org/10.1016/j.apenergy.2015.04.031.
- BP, 2024. Statistical Review of World Energy 2024. BP, London p.l.c. https://www.bp.com/en/global/corporate/energy-economics/statistical-review-of-world-energy.html.
- Bussi, G., Donadio, D., Parrinello, M., 2007. Canonical sampling through velocity rescaling. J. Chem. Phys. 126, 14101. https://doi.org/10.1063/1.2408420.
- Coskuner, G., Naderi, K., Babadagli, T., 2015. An enhanced oil recovery technology as a follow up to cold heavy oil production with sand. J. Pet. Sci. Eng. 133, 475–482. https://doi.org/10.1016/j.petrol.2015.06.030.

 Darden, T., York, D., Pedersen, L., 1993. Particle mesh ewald: an N·log(N) method
- Darden, T., York, D., Pedersen, L., 1993. Particle mesh ewald: an N-log(N) method for Ewald sums in large systems. J. Chem. Phys. 98, 10089–10092. https://doi. org/10.1063/1.464397.
- Fang, J., Wang, X., Ji, B., et al., 2024. Microscopic behavior of heteroatom asphaltene in the multi-media model: the effect on heavy oil properties. Geoenergy Sci. Eng. 241, 213180. https://doi.org/10.1016/j.geoen.2024.213180.
- Frisch, M.J., Trucks, G.W., Schlegel, H.B., et al., 2016. Gaussian 16, Revision C. 01. Gaussian, Inc., Wallingford CT.
- Gao, F., Xu, Z., Liu, G., et al., 2014. Molecular dynamics simulation: the behavior of asphaltene in crude oil and at the oil/water interface. Energy Fuel 28, 7368–7376. https://doi.org/10.1021/ef5020428.
- Gao, Y., Shen, B., Liu, J., 2013. Distribution of nickel and vanadium in Venezuela crude oil. Petrol. Sci. Technol. 31, 509–515. https://doi.org/10.1080/ 10916466.2011.576363.
- Ghatee, M.H., Shabih, M., 2017. Aggregation behavior of asphaltene of different crude oils as viewed from solution surface tension measurement. J. Pet. Sci. Eng. 151, 275–283. https://doi.org/10.1016/j.petrol.2017.01.017.
- González, M.F., Stull, C.S., López-Linares, F., et al., 2007. Comparing asphaltene adsorption with model heavy molecules over macroporous solid surfaces. Energy Fuel 21, 234–241. https://doi.org/10.1021/ef060196+.
- Guan, D., Feng, S., Zhang, L., et al., 2019. Mesoscale simulation for heavy petroleum system using structural unit and dissipative particle dynamics (SU-DPD) frameworks. Energy Fuel 33, 1049–1060. https://doi.org/10.1021/acs.energyfuels.8b04082.
- Hess, B., Bekker, H., Berendsen, H.J.C., et al., 1997. LINCS: a linear constraint solver for molecular simulations. J. Comput. Chem. 18, 1463–1472. https://doi.org/10.1002/(SICI)1096987X(199709)18:12<1463::AID-JCC4>3.0.CO;2-H.
- Horeh, N.B., Hosseinpour, N., Bahramian, A., 2023. Asphaltene inhibitor performance as a function of the asphaltene molecular/aggregate characteristics: evaluation by interfacial rheology measurement and bulk methods. Fuel 339, 127420. https://doi.org/10.1016/j.fuel.2023.127420.
- Humphrey, W., Dalke, A., Schulten, K., 1996. VMD: visual molecular dynamics. J. Mol. Graph. 14, 33–38. https://doi.org/10.1016/0263-7855(96)00018-5.
- Ji, D., Liu, G., Zhang, X., et al., 2020. Molecular dynamics study on the adsorption of heavy oil drops on a silica surface with different hydrophobicity. Energy Fuel. 34, 7019–7028. https://doi.org/10.1021/acs.energyfuels.0c00996.
- Kober, T., Schiffer, H.W., Densing, M., et al., 2020. Global energy perspectives to 2060—WEC's world energy scenarios 2019. Energy Strategy Rev. 31, 100523. https://doi.org/10.1016/j.esr.2020.100523.
- Kuznicki, T., Masliyah, J.H., Bhattacharjee, S., 2008. Molecular dynamics study of model molecules resembling asphaltene-like structures in aqueous organic solvent systems. Energy Fuel. 22, 2379–2389. https://doi.org/10.1021/ psp000573
- Lan, T., Zeng, H., Tang, T., 2019. Molecular dynamics study on the mechanism of graphene oxide to destabilize oil/water emulsion. J. Phys. Chem. C 123, 22989–22999. https://doi.org/10.1021/acs.jpcc.9b05906.
- Li, J., Xiang, B., Lu, Y., et al., 2024. Sodium citrate-sodium hydroxide synergy on remediating asphaltene-contaminated solids. Chem. Eng. J. 480, 147919. https://doi.org/10.1016/j.cej.2023.147919.
- Liu, B., Lei, X., Ahmadi, M., et al., 2024. Molecular insights into oil detachment from hydrophobic quartz surfaces in clay-hosted nanopores during steamsurfactant co-injection. Pet. Sci. 21 (4), 2457–2468. https://doi.org/10.1016/j. petsci.2024.04.004.
- Lu, T., Chen, F., 2012. Multiwfn: a multifunctional wavefunction analyzer. J. Comput. Chem. 33, 580–592. https://doi.org/10.1002/jcc.22885.
- Ma, H., Xia, S., Sun, C., et al., 2023. Novel strategy of polymers in combination with silica particles for reversible control of oil-water interface. ACS Appl. Mater. Interfaces 15, 2216–2227. https://doi.org/10.1021/acsami.2c19037.
- Mendoza de la Cruz, J.L., Castellanos-Ramírez, I.V., Ortiz-Tapia, A., et al., 2009. Study of monolayer to multilayer adsorption of asphaltenes on reservoir rock minerals. Colloids Surf., A 340, 149–154. https://doi.org/10.1016/j.colsurfa.2009.03.021.
- Mikami, Y., Liang, Y., Matsuoka, T., et al., 2013. Molecular dynamics simulations of asphaltenes at the oil-water interface: from nanoaggregation to thin-film formation. Energy Fuel 27, 1838–1845. https://doi.org/10.1021/ef301610q.

- Parrinello, M., Rahman, A., 1981. Polymorphic transitions in single crystals: a new molecular dynamics method. J. Appl. Phys. 52, 7182–7190. https://doi.org/ 10.1063/1.328693.
- Rahmati, M., 2021. Effects of heteroatom and aliphatic chains of asphaltene molecules on their aggregation properties in aromatics solvents: a molecular dynamics simulation study. Chem. Phys. Lett. 779, 138847. https://doi.org/10.1016/j.cplett.2021.138847.
- Ren, B., Xie, Z., Zhao, G., 2024. A novel quantitative evaluation method for viscosity reduction effect of heavy oil cold recovery based on the area diffusion process. J. Mol. Liq. 404, 124882. https://doi.org/10.1016/j.molliq.2024.124882.
- Schmid, N., Eichenberger, A.P., Choutko, A., et al., 2011. Definition and testing of the GROMOS force-field versions 54A7 and 54B7. Eur. Biophys. J. 40, 843–856. https://doi.org/10.1007/s00249-011-0700-9.
- Schuler, B., Meyer, G., Pena, D., et al., 2015. Unraveling the molecular structures of asphaltenes by atomic force microscopy. J. Am. Chem. Soc. 137, 9870–9876. https://doi.org/10.1021/jacs.5b04056.
- Schüppel, M., Gräbner, M., 2024. Pyrolysis of heavy fuel oil (HFO)—A review on physicochemical properties and pyrolytic decomposition characteristics for application in novel, industrial-scale HFO pyrolysis technology. J. Anal. Appl. Pyrolysis 179, 106432. https://doi.org/10.1016/j.jaap.2024.106432.
- Seidy-Esfahlan, M., Tabatabaei-Nezhad, S.A., Khodapanah, E., 2024. Comprehensive review of enhanced oil recovery strategies for heavy oil and bitumen reservoirs in various countries: global perspectives, challenges, and solutions. Heliyon 10, e37826. https://doi.org/10.1016/j.heliyon.2024.e37826.
- Shahzad, A., Zahra, A., Li, H., et al., 2024. Modern perspectives of heavy metals alleviation from oil contaminated soil: a review. Ecotoxicol. Environ. Saf. 282, 116698. https://doi.org/10.1016/j.ecoenv.2024.116698.
- Silva, H.S., Sodero, A.C.R., Bouyssiere, B., et al., 2016. Molecular dynamics study of nanoaggregation in asphaltene mixtures: effects of the N, O, and S heteroatoms. Energy Fuel 30, 5656–5664. https://doi.org/10.1021/acs.energyfuels.6b01170.
- Stroet, M., Caron, B., Visscher, K.M., et al., 2018. Automated topology builder version 3.0: prediction of solvation free enthalpies in water and hexane. J. Chem. Theor. Comput. 14, 5834–5845. https://doi.org/10.1021/acs. jctc.8b00768.
- Sun, C., Ma, H., Yu, F., et al., 2024. Preparation and evaluation of hydroxyethyl cellulose-based functional polymer for highly efficient utilization of heavy oil under the harsh reservoir environments. Int. J. Biol. Macromol. 259, 128972. https://doi.org/10.1016/j.ijbiomac.2023.128972.
- Sun, W., Liu, B., Zhang, X., et al., 2025. Analysis of wax deposition phase change law and main influencing factors in oil-water mixed transportation pipeline under unsteady working conditions. Geoenergy Sci. Eng. 245, 213475. https://doi.org/ 10.1016/j.geoen.2024.213475.
- Tazikeh, S., Shafiei, A., Yerkenov, T., et al., 2022. A systematic and critical review of asphaltene adsorption from macroscopic to microscopic scale: theoretical, experimental, statistical, intelligent, and molecular dynamics simulation approaches. Fuel 329, 125379. https://doi.org/10.1016/j.fuel.2022.125379.
- Temizel, C., Kirmaci, H., Inceisci, T., et al., 2016. Production optimization in heavy oil recovery processes. SPE Heavy Oil Conf. Exhibit. https://doi.org/10.2118/184135-ms.
- Wang, L., Hu, Y., Wang, L., et al., 2021. Visbreaking of heavy oil with high metal and asphaltene content. J. Anal. Appl. Pyrolysis 159, 105336. https://doi.org/10.1016/j.jaap.2021.105336.
- Wang, Z., Li, S., Li, Z., 2022. A novel strategy to reduce carbon emissions of heavy oil thermal recovery: condensation heat transfer performance of flue gas-assisted steam flooding. Appl. Therm. Eng. 205, 118076. https://doi.org/10.1016/j.applthermaleng.2022.118076.
- Wu, J., Li, S., Li, Q., et al., 2024. Characterization of chemical composition of high viscosity heavy oils: macroscopic properties, and semi-quantitative analysis of molecular composition using high-resolution mass spectrometry. Pet. Sci. 21 (5), 3612–3620. https://doi.org/10.1016/j.petsci.2024.02.019.
- Xiong, R., Guo, J., Kiyingi, W., et al., 2024. Technical transformation of heavy/ultraheavy oil production in China driven by low carbon goals: a review. J. Clean. Prod. 458, 142532. https://doi.org/10.1016/j.jclepro.2024.142531.
- Xu, F., Chen, Q., Ma, M., et al., 2020. Displacement mechanism of polymeric surfactant in chemical cold flooding for heavy oil based on microscopic visualization experiments. Geo-Energy Res. 4, 77–85. https://doi.org/10.26804/ager.2020.01.07.
- Xu, Y., Ayala-Orozco, C., Chiang, P.T., et al., 2020. Understanding the role of iron (III) tosylate on heavy oil viscosity reduction. Fuel 274, 117808. https://doi.org/10.1016/j.fuel.2020.117808.
- Yang, Y., Liu, D., Liang, X., et al., 2023. Influence of mineral species on oil-soil interfacial interaction in petroleum-contaminated soils. Chin. J. Chem. Eng. 61, 147–156. https://doi.org/10.1016/j.cjche.2023.02.015.
- Yatimi, Y., Mendil, J., Marafi, M., et al., 2024. Advancement in heavy oil upgrading and sustainable exploration emerging technologies. Arab. J. Chem. 17, 105610. https://doi.org/10.1016/j.arabjc.2024.105610.
- Yuan, Y., Liu, S., Yuan, S., 2023. Novel insights into the effects of asphaltenes on oil phase properties: crude oil, oil-water interface, and graphene oxide synergistic demulsification. J. Mol. Liq. 391, 123405. https://doi.org/10.1016/j. molliq.2023.123405.
- Zhang, B., Xu, C., Liu, Z., et al., 2023. Mechanism investigation of steam flooding heavy oil by comprehensive molecular characterization. Pet. Sci. 20 (4), 2554–2563. https://doi.org/10.1016/j.petsci.2023.03.018.

- Zhang, H., Liu, S., Wang, X., et al., 2022. Molecular dynamics study on emulsified oil droplets with nonionic surfactants. J. Mol. Liq. 346, 117102. https://doi.org/10.1016/j.molliq.2021.117102.
- Zhang, J., Lu, T., 2021. Efficient evaluation of electrostatic potential with computerized optimized code. Phys. Chem. Chem. Phys. 23, 20323–20328. https://doi.org/10.1039/d1cp02805g.
- Zhang, J., Zhu, B., Yuan, H., et al., 2024. Nonlinear relationship between heavy oil viscosity and asphaltene dispersion: a molecular dynamics simulation study. Chem. Eng. Sci. 295, 120173. https://doi.org/10.1016/j.ces.2024.120173.
- Zhao, C., Luan, J., Zhai, Q., et al., 2022. Releasing SiO tetrahedron and AlO octahedron from montmorillonite to enhance the adsorption performance of carbon@chitosan@montmorillonite nanosheet for cationic dyes: coupling quantum chemistry simulations with experiments. Sci. Total Environ. 851, 158174. https://doi.org/10.1016/j.scitotenv.2022.158174.
- Zhu, B., Yang, M., Yan, Y., et al., 2024. Insights into the effect of water content on asphaltene aggregation behavior and crude oil rheology: a molecular dynamics simulation study. J. Mol. Liq. 396, 124042. https://doi.org/10.1016/j.molliq.2024.124042.